

Scattering Properties of Two Cesium-133 (^{133}Cs) Atoms

A. M. Alkurdi¹, A.S. Sandouqa², and H.B. Ghassib¹

¹ Department of Physics, School of Science, The University of Jordan, Amman, Jordan

² Department of Physics and Basic Sciences, Faculty of Engineering Technology, Al-Balqa Applied University, Amman, Jordan

Abstract

The scattering properties of two ^{133}Cs atoms are investigated within the framework of the Lippmann-Schwinger (LS) formalism. Specifically, the total, viscosity and spin-exchange cross sections, for both singlet and triplet states, are computed. The LS equation is solved quite accurately by a matrix-inversion technique. Sharp resonance peaks, representing ‘quasi’ bound states, appear in these cross sections. In the triplet total and viscosity cross sections, quantum effects appear as undulations. Finally, the results obtained for the *complex* spin-exchange cross sections are particularly highlighted, because of their importance in the spectroscopy of the $^{133}\text{Cs}_2$ dimer.

Key words: Total, viscosity, and spin-exchange cross sections, Morse potential, Lippmann-Schwinger (LS) equation.

1. Introduction

This work explores the scattering properties of two interacting ^{133}Cs atoms. These properties include – for both singlet and triplet states – the total, viscosity, and (complex) spin-exchange cross sections (Dmitriev, 2014).

Cs is a boson with spin 1. Its only stable isotope is ^{133}Cs , which is hard to get in a pure condition. This is a highly-reactive alkali metal, whose boiling point is 944.0 K and melting point is 301.6 K. As a result of its large activity, it interacts strongly with air and water, the interaction being accompanied by an explosion (Kerman *et al.*, 2001).

The advent of magnetic and magneto-optical traps has made it possible to attain ultralow temperatures ($T \leq \mu\text{K}$). At such T , even heavy gases like Cs and Rb become *quantum* gases, the corresponding de Broglie wavelength becoming comparable to the interparticle spacing (Walraven, 1995). There, these gases exhibit Bose-Einstein condensation (BEC) (Anderson *et al.*, 1995; Bradley *et al.*, 1995; Davis *et al.*, 1995; Cornell and Wiemann, 2002; Ketterle, 2002).

Measurements of the various scattering cross sections for spin-polarized atomic Cs in the T -range 30-250 μK indicated clearly that these do not depend on T in this range (Monroe *et al.*, 1993). The spin-exchange cross section and the magnetic resonance frequency shift, upon collision of two Cs atoms in the ground state, were calculated using the interaction potentials for the singlet and triplet states of the Cs_2 dimer (Dmitriev *et al.*, 2014).

The starting point of this work is the choice of the Cs-Cs potential. This has been chosen to be the widely-used Morse potential (Morse, 1929) with specific parameters (Krauss and Stevens, 1990). Next, this potential, which is the basic input in the formalism, is fed into the momentum-space version of Schrödinger’s equation, namely, the Lippmann-Schwinger (LS) t-matrix integral equation (Bishop *et al.*, 1977). The t-matrix, which is the central quantity in the formalism, is calculated as a first step in computing the corresponding phase shifts which, in turn, yield the cross sections.

The rest of this work is organized as follows. In Section 2, the input potentials for the singlet and triplet states, as well as our theoretical framework, are presented. The results follow in Section 3; they are displayed in figures and tables, then discussed thoroughly and compared to previous results. Finally, the paper

closes with a general Conclusion (Section 4).

2. Theoretical Framework

2.1 Interatomic Potential

As for other atomic and molecular systems, the Cs-Cs potential is available in more than one version, depending on the methods of construction. These are all square-integrable and, therefore, Fourier-transformable. The Morse potential reads

$$V(r) = \varepsilon \exp \left[-2a \left(\frac{r}{r_e} - 1 \right) \right] - 2 \exp \left[-a \left(\frac{r}{r_e} - 1 \right) \right], \quad (1)$$

where $a = \frac{\omega_e}{2\sqrt{\beta_e \varepsilon'}}$. The parameters pertaining to both singlet and triplet states are listed in Table 1 (Dickinson and Rudge, 1970; Krauss and Stevens, 1990), and the corresponding potentials are plotted in Fig. 1.

Table 1: The Morse parameters for both singlet and triplet states (Dickinson and Rudge, 1970; Krauss and Stevens, 1990).

Parameter	Singlet	Triplet
r_e	4.625(Å)	6.265(Å)
β_e	0.0131(cm ⁻¹)	0.00597(cm ⁻¹)
ω_e	40.99(cm ⁻¹)	12.29(cm ⁻¹)
ε	5140.74(K)	406.2(K)
ε'	3573.01(cm ⁻¹)	282.32(cm ⁻¹)

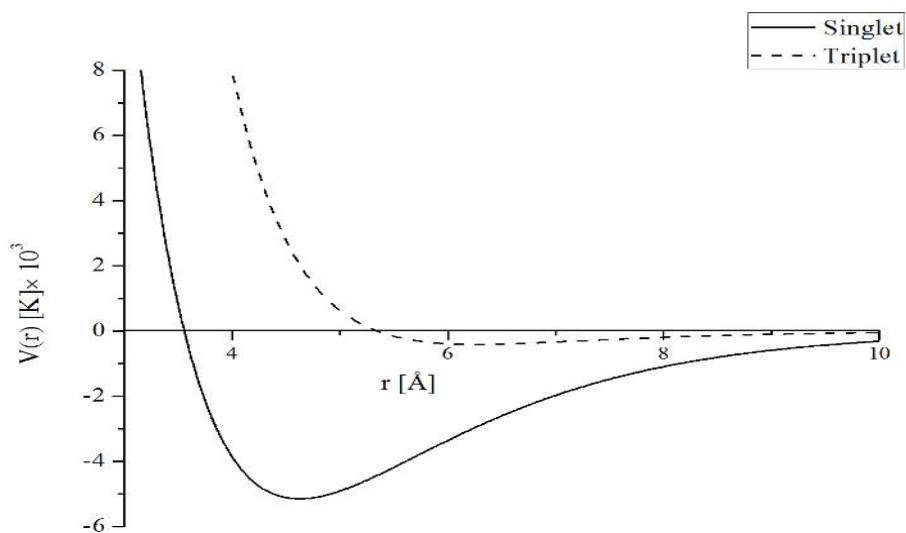


Figure 1: The Cs-Cs potential for both singlet $x^1 \Sigma_g^+$ and triplet $x^3 \Sigma_u^+$ states.

2.2 LS t-matrix

Operationally, this is given by (Landau, 1996)

$$t = u - u \frac{1}{e} t, \quad (2)$$

where u is the potential operator, and e is the ‘energy denominator’ defined below. The physical content of this equation is quite transparent: In terms of a Neumann series (Mathews and Walker, 1969) for the right-hand side, the zeroth term is just the ‘bare’ potential u . Successive terms denote the idea of multiple scattering, inherent in microscopic physics. Equation (2), then, expresses the closed sum of an infinite series. Transferring the last term on its right-hand side to the left-hand side, one can see at once that a solution for t can be obtained by matrix inversion. This technique has been brought to a fairly high level of sophistication during the past few decades (Ghassib *et al.*, 1976; Bishop *et al.*, 1977; Al-Maaitah *et al.*, 2016; Al Harazneh *et al.*, 2018).

In the momentum representation, Eq. (1) reads

$$t(\vec{p}, \vec{p}'; s, \vec{P}, \beta) = u(\vec{p} - \vec{p}') - (2\pi)^{-3} \int d\vec{k} \frac{u(\vec{p} - \vec{k}) \times t(\vec{k}, \vec{p}'; s, \vec{P}, \beta)}{k^2 - s - i\eta}. \quad (3)$$

Here: \vec{P} is the center-of-mass momentum, \vec{p} and \vec{p}' are, respectively, the incoming and outgoing relative momenta. Throughout this work, use is made of the ‘natural’ system of units, such that $\hbar = m = k_B = 1$, m being the atomic mass, \hbar Dirac’s constant ($= \hbar / 2\pi$), and k_B Boltzmann’s constant. The conversion factor for the present system is $\hbar^2/m = 0.3653 \text{ K.Å}^2$. The operator u is given by $u \equiv \frac{2m_r V}{\hbar^2} \equiv \frac{1}{2} V$ [in natural units], m_r being the reduced mass of the interacting pair: $m_r = \frac{1}{2}m$, and $V = V(p, p')$, the Fourier transform of the static, central Cs-Cs potential. The parameter s is the total energy of the interacting pair in the center-of-mass frame and is given by $s = \frac{2m_r}{\hbar^2} \left(P_0 - \frac{\hbar^2 P^2}{2M} \right)$, where (P, \vec{P}) is the corresponding four-vector momentum: $P_0 = \frac{\hbar^2 P^2}{2M} + \frac{\hbar^2 k^2}{2m_r}$, and $M = 2m$; so,

$$s = k^2. \quad (4)$$

Upon partial-wave decomposition, Eq. (3) takes the form (Bishop *et al.*, 1977)

$$t_\ell(p, p'; s, P, \beta) = u_\ell(p, p') - (2\pi)^{-2} \int_0^\infty k^2 dk \frac{u_\ell(p, k) \times t_\ell(k, p'; s, P, \beta)}{k^2 - s - i\eta} \quad (5)$$

This equation represents the ‘full off-shell’ (i.e., nondiagonal) t-matrix, pertaining to inelastic scattering, for a relative partial wave ℓ . From this, the ‘on-energy-shell’ (diagonal) counterpart $t_\ell(p, P)$, representing elastic scattering, is obtained directly by setting $p = p'$ and $s = p^2$.

The t-matrix is complex. It is, therefore, convenient to define a real K-matrix as follows:

$$K_\ell(p, p'; s, P, \beta) \equiv u_\ell(p, p')$$

$$- \frac{1}{2\pi^2} \int_0^\infty dk \frac{k^2 u_\ell(p, k; s) K_\ell(k, p'; s) - s u_\ell(p, \kappa) K_\ell(\kappa, p'; s)}{k^2 - s}, \quad (6)$$

$$\kappa \equiv \sqrt{s}.$$

Clearly, the K-matrix can readily be obtained from the t-matrix by ‘smoothing out’ the principal-value integral (Mathews and Walker, 1969) [The full details of this and other steps involved in the calculations are given in a previous work (Ghassib *et al.*, 1976)].

The relative phase shift $\delta_\ell(p)$ can now be obtained from the parametrization

$$K_\ell(p; p; p^2) = -\frac{4\pi}{p} \tan \delta_\ell(p). \quad (7)$$

The on-shell equation is an integral equation of the Fredholm kind which we have solved by matrix inversion, using Gaussian quadrature over the interval $(0, \infty)$ with an appropriate mapping. Specifically, the Gaussian points x_i in the interval $(0, 1)$ and the corresponding weights w'_i are generated by a standard subroutine. The mapping

$$q_i = \tan\left(\frac{\pi x_i}{2}\right) \quad (8)$$

transforms the mesh $\{x_i\}$ to $\{q_i\}$ in the interval $(0, \infty)$, the corresponding weights being

$$w_i = \frac{\pi}{2} (1 + q_i^2) w'_i. \quad (9)$$

2.3 Cross Sections

The main input in computing the scattering properties is the phase shift $\delta_\ell(p)$. The total cross section σ_T for ^{133}Cs - ^{133}Cs scattering is given by (Bouledroua and Zerguini, 2002; Lim and Larsen, 1981)

$$\sigma_T = \frac{1}{4} \sigma^{(1)} + \frac{3}{4} \sigma^{(3)}, \quad (10)$$

where $\sigma^{(1)} = \frac{9}{16} \sigma_{\text{odd}}^{(1)} + \frac{7}{16} \sigma_{\text{even}}^{(1)}$ and $\sigma^{(3)} = \frac{9}{16} \sigma_{\text{even}}^{(3)} + \frac{7}{16} \sigma_{\text{odd}}^{(3)}$,

Here, the superscripts 1 and 3 stand for the singlet and triplet states, respectively; $\delta_\ell^{(1)}$ and $\delta_\ell^{(3)}$ are the corresponding ℓ -partial phase shifts. $\sigma_T^{(1)}$ and $\sigma_T^{(3)}$ are the corresponding cross sections, and are given by

$$\sigma_T^{(S)} = \frac{8\pi}{k^2} \sum_{\ell} (2\ell + 1) \sin^2(\delta_\ell^{(S)}(k)). \quad (11)$$

Similarly, the effective viscosity cross section σ_η is (Cote *et al.*, 1994)

$$\sigma_\eta = \frac{1}{4} \sigma^{(1)} + \frac{3}{4} \sigma^{(3)}; \quad (12)$$

$$\sigma^{(1)} = \frac{9}{16} \sigma_{\text{odd}}^{(1)} + \frac{7}{16} \sigma_{\text{even}}^{(1)} \quad \text{and} \quad \sigma^{(3)} = \frac{9}{16} \sigma_{\text{even}}^{(3)} + \frac{7}{16} \sigma_{\text{odd}}^{(3)};$$

$$\sigma_\eta^{(S)} = \frac{4\pi}{k^2} \sum_{\ell} \frac{(\ell+1)(\ell+2)}{\left(\ell + \frac{3}{2}\right)} \sin^2(\delta_{\ell+2}^{(S)}(k) - \delta_\ell^{(S)}(k)), \quad (13)$$

Finally, the real part of the spin-exchange cross section is given by (Cote *et al.*, 1994; Dmitriev *et al.*, 2014)

$$\sigma_s^R = \frac{\pi}{k^2} \sum_{\ell=0}^{\infty} (2\ell + 1) \sin^2(\delta_\ell^{(3)}(k) - \delta_\ell^{(1)}(k)); \quad (14)$$

and the imaginary part by (Dmitriev *et al.*, 2014)

$$\sigma_s^I = \frac{\pi}{k^2} \sum_{\ell=0}^{\infty} (2\ell + 1) \sin(2(\delta_\ell^{(3)}(k) - \delta_\ell^{(1)}(k))). \quad (15)$$

3. Results and Discussion

Our results for the ^{133}Cs - ^{133}Cs total, viscosity, as well as (real and imaginary parts of) spin-exchange, cross sections are summarized in Figs. 2-4 and Table 2.

Figure 2 illustrates the behavior of the singlet and triplet total cross sections, $\sigma_T^{(1)}$ and $\sigma_T^{(3)}$, as functions of the relative momentum k . Classical theory predicts decreasing cross-section with increasing energy. This is not the case here, signaling that quantum theory has taken over. Two quantum effects are evident in the singlet total cross section $\sigma_T^{(1)}$: The first is the sharp minima-and-maxima structure. The second effect is the sharp resonance peaks. These peaks represent quasi-bound states – ‘quasi’ in the sense that the lifetime of the ‘loosely-bound’ pair of particles is not long enough for the pair to form a bound-state proper. In the triplet total cross section $\sigma_T^{(3)}$, quantum effects appear as undulations.

In general, this behavior of total cross section arises from a delicate balance between the attractive and repulsive forces; with increasing k (or energy), more and more ℓ -waves contribute ‘extra attraction’ to the scattering.

Figure 3 represents the singlet and triplet viscosity cross sections, $\sigma_\eta^{(1)}$ and $\sigma_\eta^{(3)}$, as functions of k ; σ_η has the same overall behavior as σ_T .

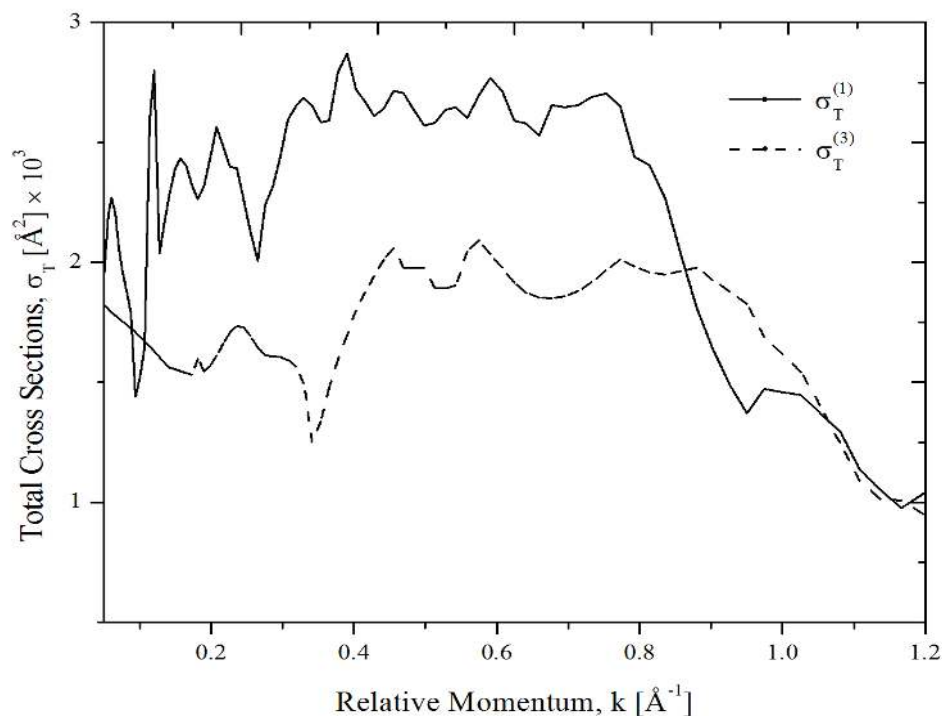


Figure 2: The total singlet and triplet cross sections, $\sigma_T^{(1)}$ and $\sigma_T^{(3)}$, for ^{133}Cs - ^{133}Cs scattering, as functions of relative momentum k [\AA^{-1}].

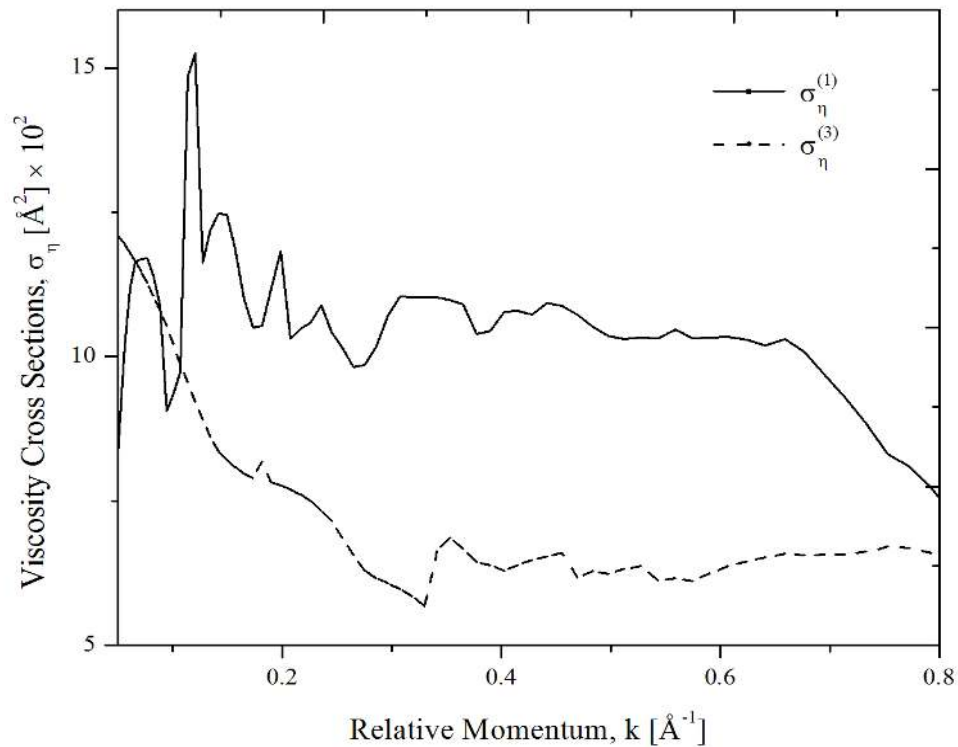


Figure 3: The viscosity cross section σ_{η} [Å²] as a function of relative momentum k [Å⁻¹].

Figure 4 shows the behavior of the real spin-exchange cross section σ_s^R , and imaginary spin-exchange cross section σ_s^I , as functions of k . This behavior is caused by the difference in the potentials for the electronic spin-singlet state V_s and triplet state V_t (Baumgarten *et al.*, 2008). Once the complex spin-exchange cross section is known, the processes occurring in spin-exchange collisions can be described completely. Specifically, σ_s^R determines the transfer of orientation during collisions of particles, relaxation times, and formation of higher polarization moments. σ_s^I determines the magnetic-resonance frequency shifts in the system of Zeeman levels as well as hyperfine atomic levels (Dmitriev *et al.*, 2014; Kartoshkin, 2015).

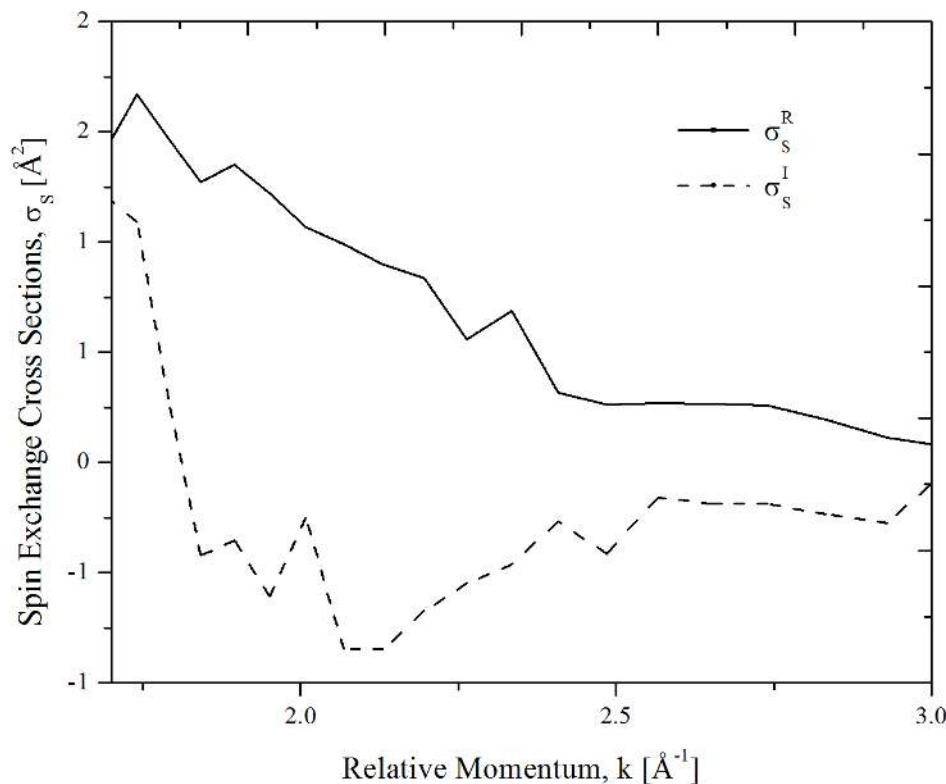


Figure 4: The spin-exchange cross sections (real and imaginary parts) [\AA^2], for ^{133}Cs - ^{133}Cs scattering, as functions of relative momentum k [\AA^{-1}].

The total and viscosity cross sections were also calculated in the limit $k \rightarrow 0$ for both singlet and triplet states (Table 2).. Further, in this limit, $\sigma_s^R = 2124.05$ [\AA^2], and $\sigma_s^I = -230599.90$ [\AA^2]. All these cross sections are quite large. This means that alkali atoms have a distinct advantage for evaporative cooling, as confirmed by using magneto-optical traps (Tiesinga *et al.*, 1992).

Table 2: Total and viscosity cross sections in the limit $k \rightarrow 0$

	Singlet State	Triplet State
$\sigma_T(0)$ [\AA^2]	1765.67	3510.51
$\sigma_\eta(0)$ [\AA^2]	1158.80	1915.86

4. Conclusion

In this paper, a comprehensive calculation was presented for the total, viscosity, and (complex) spin-exchange cross sections, in both singlet and triplet electronic-spin-states, for ^{133}Cs - ^{133}Cs scattering. The sole input was the binary potential, taken here as the Morse potential, with suitable parameters based on

experimental as well as theoretical work. The formalism was the Lippmann-Schwinger t-matrix integral equation, which was solved quite accurately using a well-tested matrix-inversion method. Whenever possible, comparison to previously published results was made; the agreement was by and large good. In particular, the singlet total and viscosity cross sections were found to exhibit the familiar sharp minima-and-maxima structure. Moreover, the equally familiar sharp resonance peaks, representing quasi-bound states, showed up in these cross sections. In the triplet cross sections, quantum effects manifested themselves as undulations. Finally, the results obtained for the *complex* spin-exchange cross sections were particularly highlighted because of their importance in the spectroscopy of the $^{133}\text{Cs}_2$ dimer.

5. References

- Akour, A.N., Sandouqa, A.S., Joudeh, B.R., and Ghassib, H.B. (2018), Equation of State of ^{20}Ne gas in the temperature-range 27–36 K, **Chinese Journal of Physics** 56(1), 411-422.
- Al Harazneh, A. A., Sandouqa, A.S., Joudeh, B. R., and Ghassib, H. B. (2018), Scattering Properties of Ground-State ^{23}Na Vapor Using Generalized Scattering Theory, **Journal of Low Temperature Physics** 192(1-2), 117–132.
- Al-Maaitah, I. F., Joudeh, B. R., Sandouqa, A. S., and Ghassib H. B. (2016), Scattering Properties of Argon Gas in the Temperature Range 87.3-120 K, **Acta Physica Polonica A** 129, 1131-1140.
- Anderson, M., Ensher, J., Matthews, M., Wieman, C. E. and Cornell, E. A. (1995), Observation of Bose-Einstein Condensation in a Dilute Atomic Vapor, **Science** 269, 198-201.
- Baumgarten, C., Braun, B., Capiluppi, M., Ciullo, G., Dalpiaz, B. F., Kolster, H., Lenisa, P., Marukyan, H., Nass, A., Reggiani, D., Stancari, M. and Steffens, E. (2008). First Measurement of the Hydrogen Spin-exchange Collision Cross Section in the Low Temperature Region, **Eur.Phys.J** 48, 343-350.
- Bishop, R. F., Ghassib, H. B., and Strayer, M. R. (1976), Composite Pairs and Effective Two-Body Scattering in a Many-Body Medium, **Physical Review A** 13(4), 1570-1580.
- Bishop, R. F., Ghassib, H. B., and Strayer, M. R. (1977). Low-Energy He-He Interaction with Phenomenological Potentials, **Journal of Low Temperature Physics**, 26 (5/6), 669-690.
- Bouledroua, M., and Zerguini, T.H. Self-diffusion properties of neutral monatomic alkali–metal plasmas (2002), **Physics of Plasmas** 9(10), 4348-4353.
- Bradley, C. C., Sackett, C. A., Tollett, J. J. and Hulet, R. G. (1995), Evidence of Bose-Einstein Condensation in an Atomic Gas with Attractive Interactions, **Physical Review Letters** 75 (9), 1687.
- Cornell, E. A. and Wieman, C. E. (2002), Nobel Lecture: Bose-Einstein Condensation in a Dilute Gas: The First 70 Years and Some Recent Experiments, **Reviews of Modern Physics** 74, 875-891.
- Cote, R., Dalgarno, A. and Jamieson, M. J. (1994). Elastic Scattering of two ^7Li atoms, **Physical Review A**, 50, 1.
- Davis, K. B., Mewes, M. O., Andrews, M. R., Van druten, N. J., Durfee, D. M., Kurn and Ketterle. W. (1995), Bose-Einstein Condensation in a Gas of Sodium Atoms, **Physical Review Letters** 75(22), 3969.

Dickinson, H. O. and Rudge, M. R. H. (1970), Total Elastic Scattering and Spin-change Cross Sections for Collisions between Alkali Atoms, **Journal of Physics B: Atomic and Molecular Physics** 3, 1448-14

Dmitriev, S.P., Dovator, N.A., and Kartoshkin, V.A. (2014), Spin Exchange upon Collision of Two Cesium Atoms in the Ground State, **Technical Physics** 60(6), 826-829.

Ghassib, H. B., Bishop, R. F., and Strayer, M. R. (1976), A Study of the Galitskii-Feynman T-Matrix for Liquid ³He. **Journal of Low Temperature Physics** 23(3-4), 393-401.

Kartoshkin, V. A. (2015), Complex Spin-Exchange Cross Sections in Collisions of Rubidium Isotopes in the Ground State, **Optics and Spectroscopy** 119(4), 594-598.

Kerman, A.J., Chin, C., Vuletic, V., Chu, S., Leo, P. H., Williams, C. J. and Julienne, P. S. (2001), Determination of Cs–Cs Interaction Parameters Using Feshbach Spectroscopy, **Molecular Physics** 85, 633–639.

Ketterle, W. (2002), Nobel Lecture: When Atoms Behave as Waves: Bose-Einstein Condensation and the Atom Laser, **Reviews of Modern Physics** 74, 1131-1151.

Krauss, M., and Stevens, W.J. (1990), Effective core potentials and accurate energy curves for Cs₂ and other alkali diatomics, **Journal of Chemical Physics** 93(6), 4236-4242.

Landau, R. (1996), **Quantum Mechanics II**. (2nd ed.), New York: Wiley.

Lim, T.K., and Larsen, S.Y. (1981), The Ramsauer–Townsend effect in molecular systems of electron-spin-polarized hydrogen and helium and their isotopes. **Journal of Chemical Physics** 74, 4997.

Mathews, J. and Walker, R. L. (1969), **Mathematical Methods of Physics**, New York: Adison-Wesley.

Monroe, C. R., Cornell, E. A., Sackett, C. A., Myatt, C. J., and Wieman, C. E. (1993), Measurement of Cs-Cs Elastic Scattering at T=30μK, **Physical Review Letters** 70, 414-417.

Morse, P.M. (1929), Diatomic Molecules According to the Wave Mechanics. **Physical Review** 34, 57-64.

Tiesinga, E., Moerdijk, A. J., Verhaar, B. J. and Stoof, H. T. C. (1992). Conditions for Bose-Einstein condensation in magnetically trapped atomic cesium, **Physical Review A** 46, R1167.

Walraven, J. T. M. (1995), Atomic hydrogen: the quantum gas. **Physics World** 8(7), 37-42.